

Document downloaded from:

<http://hdl.handle.net/10251/160594>

This paper must be cited as:

Villar-Cano, M.; Marqués-Mateu, Á.; Jiménez-Martínez, MJ. (2020). Triangulation network of 1929-1944 of the first 1:500 urban map of València. *Survey Review (Online)*. 52(373):317-329. <https://doi.org/10.1080/00396265.2018.1564599>



The final publication is available at

<https://doi.org/10.1080/00396265.2018.1564599>

Copyright Maney Publishing

Additional Information

# Triangulation Network of 1929-1944 of the First 1:500 Urban Map of València

M. Villar-Cano, A. Marqués-Mateu and M.J. Jiménez-Martínez  
Department of Cartographic Engineering, Geodesy and Photogrammetry,  
Universitat Politècnica de València  
Camino de Vera s/n, 46022 València, Spain  
Corresponding author: M.J. Jiménez-Martínez  
E-mail address: mjjimenez@cgf.upv.es (M.J. Jiménez-Martínez).

## Abstract

1        Triangulation is a surveying method on which earlier maps made were based.  
2        Although the origins of the method can be traced back to the 16<sup>th</sup> century, it is  
3        still used today, with minor changes, to adjust networks observed with modern  
4        geodetic techniques. In this paper we present the geodetic survey work that was  
5        carried out for the primary triangulation network of the first 1:500 urban map of  
6        the city of València (Spain). It spanned from 1929 to 1944 and resulted in 421  
7        maps covering about 174 square kilometres. We focus on four key elements to  
8        define the geometric framework of a map: (1) the geodetic network, (2) the  
9        cartographic projection, (3) the baseline measurements, and (4) the primary  
10       triangulation. The paper is based on the interpretation of original documents and  
11       field books recovered from the archives of the València City Council. In order to  
12       check the accuracy and consistency of the survey work, we recomputed all  
13       calculations directly from the field data, following the mathematical procedures  
14       of the time. We obtained a set of transformation parameters to convert the  
15       coordinates of 1929 to current coordinates based on the European Terrestrial  
16       Reference System of 1989 (ETRS89). Results showed that the 1929 primary  
17       triangulation angles and coordinates are accurate to 8" and 35 cm respectively,  
18       and that the coordinates transform well into the current reference system with  
19       average residuals of 26 cm across nine control points, demonstrating the high  
20       quality of the 1929 work.

21  
22       Keywords: urban mapping, triangulation, cartographic heritage, quality control,  
23       geodetic surveying, ETRS89

## 25    1. Introduction

26    In 1929, the València City Council commissioned the Instituto Geográfico y Catastral  
27    (IGC), the former Spanish National Mapping Agency, to make the first accurate urban

28 map at a scale of 1:500. This was quite a challenging technical endeavour at the time.  
29 The project took 15 years to complete, with an intervening civil war. València is located  
30 on the Mediterranean coast of Spain next to the mouth of the river Turia (Fig. 1) and has  
31 been historically the third city in Spain, temporarily becoming the capital of the country  
32 during the civil war. In the beginning of the 20th century, social and economic forces  
33 demanded further signs of development and modernity that had already been started  
34 with the celebration of the Regional Expo in 1909 and the inauguration of the new  
35 railway station in 1917. One key element that had to support those developments was a  
36 new urban map of the city, whose backbone was the triangulation network.

37 [Figure 1 near here]

38 The first use of the triangulation method in geodetic networks is usually  
39 attributed to the Dutch astronomer Willebrord Snel van Royen (Haasbroek 1968,  
40 Murdin 2009, Shank 2012). Snel, sometimes spelled as Snell after his latinised name  
41 Snellius, carried out a triangulation in 1615 with the purpose of finding the diameter of  
42 the earth. However, there are earlier references that include either theoretical definitions  
43 or practical applications of the method of triangulation. Indeed, it seems that Snel  
44 learned this method from publications by the Dutch cartographer and mathematician  
45 Gemma Frisius (Haasbroek 1968, Hewitt 2011), among whose students was the great  
46 cartographer Gerardus Mercator. The main reference by Frisius regarding triangulation  
47 was *Cosmographia Petri Apiani*, published in 1533, which contained an appendix  
48 defining the method of triangulation.

49 Much less known are the early works of the Spaniard Jerónimo Muñoz who used  
50 a triangulation sketch on the Valencian coast (Fig. 2) in his university lectures. It is  
51 thought that this graphical triangulation, made in 1568 without the help of trigonometric  
52 or logarithmic calculations, and known afterwards through Snel, was the basis for the

53 creation of the Ortelian Valencian Map in 1585. It is considered a modern map with  
54 correct geodetic references, at the same technological level as other contemporary maps  
55 from nearby European countries (Navarro 2004, Roselló 2000, Roselló 2008).

56 In 1929 the method of triangulation had evolved since its inception four  
57 centuries earlier, but was still in the pre-computer era. This means that computations  
58 had to be done by manual methods, with the use of logarithm tables, thus eliminating  
59 any possibility of automation. The standard procedure was to establish two baselines at  
60 the limits of the surveyed area. Once the baselines were measured and orientated, a  
61 chain of triangles, the triangulation network proper, had to be designed to connect both  
62 baselines. After computing all triangles from the starting baseline, the computed length  
63 and azimuth for the closing baseline were available. The comparison of the measured  
64 and the computed values of this baseline determined the quality of the network and,  
65 most importantly, the scale and the orientation of the resulting map.

66 [Figure 2 near here]

67 It should be noted that the map obtained from the network of 1929 was a high  
68 class product of its time. This map was routinely used for urban planning and public  
69 information purposes until the 1990s, and even later, in several city council services.  
70 The 1929 map is still the most reliable source for graphical information on older real  
71 estate properties, roads, railways, sewer lines and other public facilities.

72 Therefore, this map must be considered as a valuable cartographic heritage item  
73 to be preserved. It should be made available to interested users, including general public  
74 users as well as researchers. In fact, urban development studies are potential candidates  
75 to extract new insights from such documents (Gatta 2010). In this line of research, the  
76 International Cartographic Association (ICA) created in 2007 the Commission on

77 Digital Technologies in Cartographic Heritage, whose aim is to encourage digital  
78 approaches to cartographic heritage (Bitelli et al. 2014).

79 The main purpose of this paper is to report on field and mathematical procedures  
80 that defined the geodetic triangulation network of the map. A second, though not less  
81 important, goal of the paper is to keep a record of the standard surveying procedures  
82 existing in the first half of the 20<sup>th</sup> century, and preserve that information for future  
83 generations of cartographers and scholars.

## 84 **2. Description and analysis of the triangulation**

85 In this section we provide the basic elements, formulas and terminology to conveniently  
86 follow the calculations given below. Triangulation has been used to define national  
87 mapping programmes in many countries (Ogilvie 1921, Adams 1940, Culley 1940,  
88 Staack 1940, Schofield & Breach 2007) using a hierarchical structure based on a  
89 primary network that is densified into several lower order networks, typically until the  
90 third or fourth order (Blachut et al. 1979). The network discussed herein must be  
91 considered as a fourth order or local network according to this classic approach. Modern  
92 techniques, especially space geodesy, have made this approach obsolete.

93 Triangulation is a well-known surveying technique that relies on the  
94 measurement of the inner angles of a triangle network with the aim of determining the  
95 distances between the stations by trigonometry. This method requires that one or more  
96 baselines with known lengths and azimuths be measured separately to define the scale  
97 and orientation of the network (Gorse et al. 2012). In the end, the triangulation method  
98 provides spatial locations for every station in a plane coordinate system. Moreover, the  
99 three interior angles in each triangle allow for the checking of measurement errors  
100 (Brinker & Minnick 1987). In summary, a triangulation project requires a number of

101 interconnected triangles covering the mapping area whose angles are observed using  
102 typical surveying equipment.

### 103 ***2.1. Coordinate reference system***

104 The lack of standards in 1929 led each country to adopt different local coordinate  
105 reference systems. In Spain, there were indeed several coordinate systems that were  
106 used simultaneously. Although the International Meridian Conference that defined  
107 Greenwich as the standard prime meridian had been held in 1884 in Washington, the  
108 use of a different prime meridian in each country was still common practice. In Spain,  
109 the geographic coordinates of the national geodetic network were computed using the  
110 so-called Madrid datum (Mugnier 2000), which was based on the prime meridian  
111 defined in the Madrid Astronomical Observatory ( $3^{\circ} 41' 15.45''$  west of Greenwich) and  
112 the Struve ellipsoid (IGC, 1928). The fieldwork reported in this paper was still based on  
113 the Spanish datum, even though the Greenwich meridian had officially been adopted in  
114 Spain in 1901.

115 In geodetic terms, an urban network is a lower order (4<sup>th</sup> order) or local network  
116 that needs to be geometrically connected to higher order networks to be consistent with  
117 national reference systems. Such a connection is achieved by including several high  
118 order stations in the urban network design, observation and computation. According to  
119 the documentation located for our study, the connecting network, which was executed  
120 prior to 1929, comprised 12 stations (Fig. 3), two of which (Miguelete and Almàcera)  
121 were also used in the urban network.

122 We did not find specific information on the geodetic coordinate reference  
123 system used in the project, although it was not difficult to guess. The hint was a listing  
124 containing three geodetic stations located outside of the working area with geographical  
125 and plane coordinates. We assumed that the geographical coordinates were in the

126 Madrid datum and tried several projections. It turned out that the projected coordinates  
127 were computed using the Tissot projection (Cebrián & Los Arcos 1895, Tissot 1881)  
128 still used in 1929.

129         It is not clear why this connecting network (see Fig. 3) was included in the files  
130 of the 1929 map. In theory, those networks were intended to transfer the coordinate  
131 reference system (specifically origin, scale and orientation) from the higher to the lower  
132 order network. However, the final decision was to use a local reference system with an  
133 arbitrary origin and astronomical orientation (see details in Section 2.3 and Section 4).  
134 Maybe, the information on this geodetic network was collected by the engineers from  
135 an early IGC project for the definition of the new urban coordinate system. But for  
136 some reason it was finally dismissed.

137 [Figure 3 near here]

## 138 **2.2. Baseline length**

139 There were two baseline measurements in the triangulation project of 1929. The  
140 measurement stage comprised the length and the orientation determinations of the  
141 baselines which were conducted independently from the angle observations in the  
142 network. In the beginning of the 20<sup>th</sup> century the use of rigid bars was common for  
143 baseline measuring apparatus until the advent of the invar wires technology. Invar  
144 devices were introduced in Spain by 1924 (de la Puente, 1925) and used in the 1929  
145 project. Invar is an alloy made of nickel (36%) and iron (64%) that has a uniquely low  
146 thermal expansion coefficient. Its invention dates back to the experiments conducted by  
147 Benoît and Guillaume in 1896 (Benoît & Guillaume 1917).

148         Previously in 1880, Jadörin established a new methodology to stretch metal  
149 wires which was then used to manufacture invar measurement equipment. Both  
150 inventions allowed geodesists to dramatically reduce the time required for distance

151 measurements while increasing the accuracy. The paramount role of the invar  
152 measurement technique was explained in the lecture entitled ‘Invar and elinvar’, given  
153 by Guillaume when he was awarded the Nobel Prize in 1920 (Nobel Foundation 1998).  
154 The prize was awarded ‘in recognition of the service he has rendered to precision  
155 measurements in Physics by his discovery of anomalies in nickel steel alloys.’

156 The invar measurement technique requires a division of the baseline in sections  
157 that are measured sequentially and added up to obtain the total baseline length. All the  
158 sections must be perfectly aligned with auxiliary equipment to give reliable results. The  
159 nominal length of the invar wire is 24 m, its diameter is 1.65 mm and its circular cross  
160 section is 2.14 mm<sup>2</sup> (Bomford 1952). The auxiliary equipment included a clinometer to  
161 read the slope angles, a thermometer to compute the thermal coefficient of the wires,  
162 target devices mounted on tripods to make readings against an index, a spring balance  
163 and tension poles.

164 The measurement procedure gives the length of each section in 3D space. The  
165 raw measurement ( $L_0$ ) is first corrected for the observation temperature (IGE 1907):

$$L = L_0 \cdot [1 + (0.0618 \cdot (t - t_{REF}) - 0.00065 \cdot (t - t_{REF})^2) \cdot 10^{-6}] \quad [1]$$

166 where  $L$  is the corrected measurement,  $L_0$  is the field observed measurement,  $t$  is the  
167 observation temperature and  $t_{REF}$  is the reference calibration temperature (here 15°C).  
168 This length should then be projected onto the horizontal plane using the formula:

$$L' = L \cdot \cos C_t \quad [2]$$

169 where  $L$  is the corrected slope length and  $C_t$  is the slope angle. The sum of all the values  
170 of  $L'$  amounts to the total baseline length. In order to avoid gross errors, each section



171 was measured a number of times (five times in the project of 1929). The sample of  
172 observations provides a residual ( $v_i$ ) per individual measurement:

$$v_i = L_m - L_i \quad [3]$$

173 where  $L_m$  is the average value of the series and  $L_i$  is the  $i^{\text{th}}$  measurement. The standard  
174 procedure also gives a formula to compute the standard deviation ( $s_{L_i}$ ) of a single  
175 distance measurement for every section of the baseline:

$$s_{L_i} = \sqrt{\frac{\sum_{i=1}^n v_i^2}{n - 1}} \quad [4]$$

176 The standard deviation of the mean of five measurements for each section computes as:

$$s_{\bar{L}_i} = \frac{s_{L_i}}{\sqrt{5}} \quad [5]$$

### 177 **2.3 Baseline orientation**

178 The angular orientation with respect to a standard reference line is one of the basic  
179 operations in any topographic survey. Historically, map orientation tasks have been  
180 made by astronomical observations that provide the azimuth, that is the clockwise angle  
181 from geographic north, of one or more baselines. Then, the orientation was carried  
182 forward towards the rest of the map elements through the field survey work (Bennett &  
183 Freislich 1979).

184 In the project of 1929, the orientation was conducted by the method of Polar star  
185 observations which allows obtaining the azimuth of the baseline with respect to the  
186 local meridian, or south-north line, and therefore the orientation of the map. We  
187 recreated the procedure recommended by the astronomic branch of the IGC back in  
188 1929. The procedure requires an astronomic almanac containing star ephemerides in

189 tabular format. After some bibliographic research, we found a copy of the almanac used  
190 in 1929 published by the IGC (1928).

191 The computation consists basically of solving a spherical triangle whose corners  
192 are the astronomic pole (P), the local zenith (Z) and the observed star (S). The sides of  
193 the *PZS* triangle are the Polar star zenith distance  $z = 90 - h$ , colatitude  $c = 90 - \phi$ ,  
194 and Polar distance  $p = 90 - \delta$ , where  $h$  is the altitude,  $\phi$  is the latitude of the station  
195 point, and  $\delta$  is the Polar star declination, which are all positive numbers when the  
196 station point and the observed star are on the same astronomic hemisphere.

197 The azimuth angle  $\theta$  is calculated for each polar observation in the field  
198 observation series with the following formula:

$$\tan \theta = \frac{\sin H}{\sin \delta \cdot \cos H + \tan \delta \cdot \cos \phi} \quad [6]$$

199 Thus, the determination of the azimuth requires observations of the hour angle  
200 ( $H$ ) of the Polar star, together with the values of the Polar star declination  $\delta$  and the  
201 latitude  $\phi$  of the station point.  $H$  is the inner angle at the Pole in triangle *ZPS*, also called  
202 the local time angle or hour angle, and provides the time difference of the star position  
203 at observation time with respect to the local meridian of the observer. The  $H$  angle value  
204 to be taken for computational purposes in Eq. (6) is that corresponding to the mean of  
205 the corrected chronometer times of the  $n$  observations forming a set (Clark 1948).

206 The other two parameters in Eq. (6) are known beforehand. The polar declination value  
207 used in the computations was  $\delta = 88^\circ 55' 12''$  as published in the almanac (IGC, 1928)  
208 and the latitude was  $\phi = 39^\circ 28' 30''$  N known from previous national geodetic  
209 campaigns. The uncertainty in the measurement of the hour angle propagates into the  
210 value of the computed azimuth. Assuming that the observed hour angle ( $H$ ) is in error  
211 by  $\Delta H$ , the error in the azimuth angle ( $\theta$ ) (both quantities in the same units, for instance

212 seconds of arc), may be easily obtained by differentiating the formula in Eq. (6) with  
213 respect to  $H$ . After some simplifications the error formula reduces to (Clark 1948):

$$\Delta \theta = -(\sin \phi - \cos \phi \cdot \cos \theta \cdot \tan h) \cdot \Delta H \quad [7]$$

214  
215 **2.4. Triangulation**

216 The 1929 primary triangulation comprised 28 triangles and 23 triangulation  
217 stations (Fig. 4). The observation was carefully planned to achieve quasi-equilateral  
218 triangles following the instructions of the IGE (1907). The computation was done using  
219 plane surveying procedures given the extent and the topography of the area.

220 The location of the stations was a key issue in 1929 since the instruments used  
221 back then needed clear lines of sight. The engineers of the time selected a number of  
222 elevated sites as triangulation points, mainly building rooftops and bell towers, to  
223 achieve good visibility. All stations were described and identified in specific forms (Fig.  
224 5). Those documents are very accurate and contain text and graphical information to  
225 locate the exact station point; however, most of the marks have been lost over the years.  
226 After an exhaustive search, we found nine stations which were then used to conduct  
227 further geometric analyses (see Sections 3 and 4).

228 The angular observation procedure used in the 1929 field work is described in the  
229 instruction manual of the *Instituto Geográfico y Estadístico* (IGE 1907). The field notes  
230 indicate that two sets (arcs) of directions were measured at the stations, with each set in  
231 two faces, following the standard procedure of ‘direction measurements’ (Kahmen &  
232 Faig 1988). For our computations, we extracted the required angles from the mean  
233 directions of all sets measured at stations that were reported in field notes.

234 [Figure 4 near here]

235 [Figure 5 near here]

236 The computations were done originally by hand with the help of logarithm tables  
 237 (Schrön 1893). In order to check for errors in the computations, we wrote a computer  
 238 program that simulates each step of the manual procedure and found no errors. As for  
 239 the accuracy of the primary triangulation, we recomputed the direction measurements  
 240 directly from field data and adjusted the angles using the least squares method.  
 241 Although the least squares technique is most often associated with high precision  
 242 surveying, it can be used for quality control by processing sets of redundant  
 243 observations according to mathematically well-defined rules (Kennie & Petrie 2010,  
 244 Leick et al. 2015).

245 Theoretically, all angles of a triangulation should be processed together by least  
 246 squares to yield simultaneously their most probable values (Clark 1948). We processed  
 247 the angle observations from 13 selected stations and created a redundant equation  
 248 system of dimensions 30x20, where the number of rows (30) equals the number of  
 249 angles and the number of columns (20) is the number of coordinates to be adjusted.

250 Each angle generates an independent equation comprising three points  $i, j$  and  $k$   
 251 as follows (Teunissen 2006):

252

$$\begin{aligned}
 d\alpha_{ijk} = & \frac{y_j^o - y_i^o}{(l_{ij}^o)^2} dx_j - \frac{y_j^o - y_i^o}{(l_{ij}^o)^2} dx_i - \frac{x_j^o - x_i^o}{(l_{ij}^o)^2} dy_j + \\
 & + \frac{x_j^o - x_i^o}{(l_{ij}^o)^2} dy_i - \frac{y_k^o - y_j^o}{(l_{ij}^o)^2} dx_k + \frac{y_k^o - y_j^o}{(l_{ij}^o)^2} dx_j + \\
 & + \frac{x_k^o - x_j^o}{(l_{jk}^o)^2} dy_k - \frac{x_k^o - x_j^o}{(l_{jk}^o)^2} dy_j = \alpha_o - \alpha_{ca}
 \end{aligned} \tag{8}$$

253 where  $i$  denotes the left target,  $j$  is the instrument station,  $k$  is the right target,  $dx_i, dx_j,$   
 254  $dx_k, dy_i, dy_j, dy_k$  are the unknowns (corrections to approximate coordinates),  
 255  $x_i^o, x_j^o, x_k^o, y_i^o, y_j^o, y_k^o$  are the approximate coordinates, and  $\alpha_o, \alpha_{ca}$  are the observed  
 256 and calculated angle values respectively.

257           The least squares adjustment requires approximate coordinate values for each  
 258 unknown station to calculate all parameters in Eq. (8). We used the coordinate values  
 259 reported in the original documentation as approximations. The coordinates were  
 260 computed using a set of ‘corrected angles’ that were obtained for every triangle by  
 261 adding up the values of the three inner angles, then calculating the difference with  
 262 respect to 180°, and finally distributing the angular misclosure equally to all three  
 263 angles.

264           The matrix form of the equation system and its solution is well-known (Leick et  
 265 al. 2015, Strang & Borre 1997):

$$A \cdot x = b + v \quad [9]$$

266 where  $A$  is the coefficient matrix,  $x$  is the vector of unknowns,  $b$  is the vector of  
 267 independent terms, and  $v$  is the vector of residuals. The least squares method allows  
 268 specific weighting for every observation equation. Since we did not find any  
 269 suggestions for a weighting, we computed the adjustment with equally weighted  
 270 observations:

$$x = (A^T \cdot A)^{-1} \cdot A^T \cdot b \quad [10]$$

271           The vector  $x$  of the unknowns gives the corrections to the initial  
 272 approximations of the coordinates. The most interesting point of the least squares  
 273 method with respect to the approximate methods used in 1929 is the calculation of the  
 274 variance-covariance matrix which contains the precision information of the variables.  
 275 The expression of the variance-covariance matrix ( $\Sigma_x$ ) is:

$$\Sigma_x = \sigma_o^2 \cdot (A^T \cdot A)^{-1} \quad [11]$$

276 where  $\sigma_o^2$  is the a posteriori variance of unit weight which is computed using the  
 277 following formula:

$$\sigma_o^2 = \frac{v^T \cdot v}{n - u} \quad [12]$$

278 where  $v$  is again the vector of residuals,  $n$  is the number of equations (observations),  
 279 and  $u$  is the number of unknowns. In network theory, the expression  $n - u$  is usually  
 280 referred to as the degrees of freedom of the network which equals the number of  
 281 redundant equations in the model.

282 As mentioned in Section 1, there was no least squares adjustment to calculate the  
 283 variances of the unknowns in the project of 1929. However, the triangle misclosures in  
 284 the network may be used to estimate the overall angular precision of triangulations such  
 285 as that of 1929. The classical literature provides the Ferrero equation as a means to  
 286 compute the accuracy  $s_\alpha$  of the observed angles in triangulation projects (Bomford  
 287 1952):

$$s_\alpha = \sqrt{\frac{\sum \varepsilon_i^2}{3 \cdot n}} \quad [13]$$

288 where  $n$  is the number of triangles, and  $\varepsilon_i$  is the misclosure in triangle  $i$ . It is worth  
 289 noting here that this experimental formula is intended to calculate approximate probable  
 290 errors in unadjusted triangulations from the angular measurements (Clark 1948). The  
 291 value of the  $s_\alpha$  value will be discussed later in relation to the precision of the theodolite  
 292 used and the a posteriori variance of unit weight  $\sigma_o^2$  in Section 4.2.

### 293 **3. Transformation of the 1929 network to ETRS89**

294 An interesting and challenging task of the present study was how to transform the 1929  
 295 network into a modern coordinate reference system such as the European Terrestrial  
 296 Reference System of 1989 (ETRS89), which is the official system in Spain since 2012.  
 297 We had some cues, such as the relative error of the original baseline data and the least

298 squares adjustment results, which suggested the high quality of the data, and thereby  
299 promised good transformation results (Section 4.4). However, there was a practical  
300 limitation when selecting the control points for the transformation. After preliminary  
301 field work, we found that all stations of the southern half of the area, and some others in  
302 the central (urban area) and north area were lost. We were able to find nine points that  
303 have survived almost 90 years (Fig. 6), most of them pertaining to the primary network.  
304 [Figure 6 near here]

305         The input data of a coordinate transformation consists of several pairs of  
306 coordinates in the source (1929) and target (ETRS89) coordinate systems, each pair  
307 representing some sort of transformation vector between the two spaces. While we had  
308 the source data from the published coordinates of 1929 ( $X_{1929}$  and  $Y_{1929}$  in Table 4), we  
309 did not have any information on the target system. In consequence, we had to do  
310 fieldwork to survey the target coordinates for every control point. Eight original marks  
311 were easily located following the descriptions in the project documentation. Seven  
312 marks were stations of the primary network (Grao, Castellar, Mislata, Almàcera,  
313 Benimàmet, Sancho, and Miguelete II), whereas the other two were stations of second  
314 order traverses (Puente del Mar and Petxina).

315         We collected ETRS89 coordinates using global navigation satellite system  
316 (GNSS) equipment. Specifically, we used the virtual reference station (VRS) technique  
317 because it allows short observation lengths and requires no post-processing. VRS  
318 provides instant access to real-time kinematic (RTK) corrections utilising a network of  
319 permanent (fixed), continuously operating reference stations (Leick et al. 2015, Seeber  
320 2003).

321         GNSS provides geographical coordinates ( $\phi$ ,  $\lambda$ ) of the station points in the  
322 ETRS89 coordinate reference system. In order to be more compatible with the original

323 Euclidean 2D system of 1929, the geographical coordinates were transformed to linear  
 324 coordinates expressed in metres. Using well-known formulae (Snyder 1987, Wolf et al.  
 325 2014) we converted the geographical coordinates into two coordinate systems: (1) the  
 326 Universal Transverse Mercator (UTM) projection, which is the official map projection  
 327 in Spain, and (2) a local 3D three dimensional vertical coordinate (LVC) system which  
 328 is geometrically defined in very similar terms to those of the original 1929 triangulation,  
 329 namely a 3D rectangular system with the  $z$ - axis parallel to the local vertical and the  $y$ -  
 330 axis pointing North.

331 The subsequent conversion of the 1929 coordinates to the two contemporary  
 332 coordinate sets (UTM and LVC) was conducted with an affine transformation. We  
 333 chose the affine transformation because it is very flexible and allows a detailed analysis  
 334 of the conversion. The formulas of the six-parameter affine transformation are well-  
 335 known (Wolf et al. 2014):

$$X_2 = A \cdot X_1 + B \cdot Y_1 + C \quad [14]$$

$$Y_2 = D \cdot X_1 + E \cdot Y_1 + F \quad [15]$$

336 where  $(X_1, Y_1)$  and  $(X_2, Y_2)$  are coordinates in the source and target systems  
 337 respectively. Two of the six parameters  $A, B, C, D, E$  and  $F$  have a direct geometrical  
 338 meaning ( $C$  and  $F$  represent coordinate shifts or translations). The other four parameters  
 339 can be expressed in terms of scale factors and rotations of the axes. The formulas to  
 340 obtain the scales and rotations are (Wolf et al. 2014):

$$\theta = \arctan\left(\frac{D}{A}\right) \quad [16]$$

$$\epsilon = \arctan\left(\frac{B}{E}\right) + \theta \quad [17]$$



$$SF_x = \frac{A}{\cos \theta} \quad [18]$$

$$SF_y = E \cdot \frac{\cos \epsilon}{\cos(\epsilon - \theta)} \quad [19]$$

341  
342 where  $SF_x$  and  $SF_y$  are the scale factors in  $X$  and  $Y$  directions,  $\epsilon$  is the correction for  
343 non-orthogonality between the  $x$ - and  $y$ -axes, and  $\theta$  is the rotation angle of the  $x$ -axis.  
344 The  $(\epsilon - \theta)$  difference may be interpreted as the rotation angle of the  $y$ -axis.

#### 345 346 **4. Results and discussion**

347 In this section we argue that the map of 1929, backed by a number of precise geodetic  
348 operations described in this paper, was a first class surveying project. We base our view  
349 on careful analyses of the original fieldwork records, as well as on exhaustive  
350 recomputations relating to the geodetic reference system, baseline measurements,  
351 triangulation adjustment, and geometric transformations.

##### 352 ***4.1. Geodetic coordinate system***

353 As reported above, the only reference to a proper geodetic reference system in this  
354 project was a list of coordinates in an unidentified system found in the project files.  
355 After trying several projection formulae sets, we found out that they were Tissot  
356 coordinates. Table 1 contains the coordinates listed in the 1929 project documentation  
357 together with our own Tissot computations from the original data and the differences  
358 between the two datasets. Although the computed coordinates are close to those  
359 reported in the 1929 dossier, there is a systematic shift in the  $x$ -axis, probably owing to  
360 computation procedures of the time. While we are pretty sure that the original listing  
361 contains Tissot coordinates, the reference system adopted finally was a different one as  
362 discussed below.

363 [Table 1 near here]

364 **4.2. Baselines**

365 The baselines (*AB* and *CD* in Fig. 4) gave orientation and scale to the 1929 urban map.  
366 Astronomic azimuth measurements were conducted according to the instructions  
367 defined by the IGC (1928). Each azimuth was determined twice, in opposite directions  
368 to avoid gross errors. The values reported in the project files were  $\theta_A^B = 139^\circ 03'17''$ ,  
369  $\theta_B^A = 319^\circ 03'29''$  for the baseline *AB* and  $\theta_C^D = 351^\circ 11' 35''$ ,  $\theta_D^C = 171^\circ 11'30''$  for  
370 the baseline *CD*. The differences between the reverse observations were 12'' and 5'' for  
371 the two baselines and demonstrate the accuracy of the method. The computation report  
372 of the project also contains the difference between the observed (astronomic) azimuth  
373 and the computed (carried forward from *AB*) azimuth of the baseline *CD*. That  
374 difference was 3'17'' which is another indicator of the quality of the observational  
375 scheme of the 1929 network.

376 As for the baseline measurements, the execution of the invar wire measurements  
377 provided an estimation of the precision of each section. The project files contain  
378 observation data for the *CD* baseline only, although similar precision values should be  
379 expected for the baseline *AB*. The length values reported in the documentation were  
380 508888.627 mm for *AB* and 524362.716 mm for *CD*. The final coordinates of the  
381 terminals *A*, *B*, *C* and *D* are given in Table 2. We computed the standard deviations of  
382 each single measurement as well as of the mean of every group of five observations  
383 according to the instructions published by the IGE (1907). The standard deviations for  
384 the mean values of all sections of the baseline *CD* ranged from 0.0045 mm to 0.0656  
385 mm. Using the propagation law of variances we derived the precision of the whole  
386 length of 524362.716 mm as 0.17 mm (0.32 ppm). It is worth noting that this  
387 computation covers the precision of the invar measurements only. Classic references in  
388 the geodetic literature introduce the concept of 'probable errors' as a measure of the

389 influence of all other measurement and reduction errors. For instance, Bomford (1952)  
390 quotes typical values of 1-2 ppm for the total error budget of baselines for higher order  
391 networks and gives the following formula for the probable error of measurements:

$$pe = \sigma \cdot 0.6745 \quad [20]$$

392 where  $\sigma$  is the standard deviation of the invar measurement. Given the precision of the  
393 1929 invar measurements (0.17 mm), the probable error of the raw distance  
394 measurements equates only 0.114 mm. Other error sources are likely larger (Bomford,  
395 1952).

396 [Table 2 near here]

397 The primary triangulation network (Fig. 4) may be considered as a triangulation  
398 chain of 16.94 km length from the baseline *AB* to the baseline *CD*. In consequence,  
399 there are two length values for *CD*, the direct invar measurement (524.363 m) and the  
400 computed value (524.510 m) carried forward from *AB*. The difference between the  
401 measured and the computed lengths is 0.147 m, which is quite good considering the  
402 instruments of the time.

403 The ratio of the baseline *CD* difference (0.147 m) to the distance (16.94 km)  
404 between the two baselines gives some sort of 'kilometric error' of the method. This  
405 error in the 1929 network amounts to 8.7 mm per km, or 8.7 parts per million (ppm).  
406 Some contemporary triangulation projects report relative errors ranging from 1 ppm to  
407 13.1 ppm (Hotine, 1939). Therefore the resulting value of 8.7 ppm in the 1929 project  
408 conforms to common practice of the time and must be considered a satisfactory result.

409

#### 410 ***4.3 Triangulation network***

411 The least squares adjustment of the network shown in Fig. 4 gave very good results  
412 (Table 3). The original 1929 network extends 13.4 km NS and 7.7 km EW. Due to

413 practical constrains, the network used to conduct the adjustment covers a reduced area  
 414 of 8.9 km NS and 7.7 km EW.

415 We fixed the stations Benimàmet, Miguelete I and Miguelete II based on a  
 416 previous field study. The vector of unknowns gave very small coordinate corrections  
 417 and the residuals of the angles were also small. Probably, the most interesting output of  
 418 the least squares adjustment were the standard deviations of the coordinates and the  
 419 angles. It is clear from Table 3 that the standard deviations  $s_x$  and  $s_y$  of the coordinates  
 420 increase from the first station Burriel (0.023 m) to the last station Castellar (0.354 m).  
 421 This increase of the standard deviation of the coordinates from North to South is  
 422 expected since the three fixed stations are in the North. We based our choice of the three  
 423 fixed points on previous work. In consequence, the southern part lacks geometric  
 424 control leading to higher standard deviations. Still, the adjustment results agree well  
 425 with the standards of 1929 for the geodetic control of large scale urban maps. .

426 [Table 3 near here]

427 The least squares analysis also gives the *a posteriori* variance of an observation  
 428 of unit weight  $\sigma_o^2$  as 63.97 (Eq. (12)). Thus, the *a posteriori* standard deviation  $\sigma_o$  of the  
 429 measured angles was 8 seconds of arc. The triangle misclosures computed in 1929 from  
 430 triangles 1 to 10 (Fig. 4) were: 7, 8, 9, 1, 17, 3, 9, 21, 29 and 11 seconds of arc  
 431 respectively. Substituting these values into Eq. (13) provides an estimate of the overall  
 432 angular precision  $s_\alpha$  in the network:

$$s_\alpha = \sqrt{\frac{\sum(7^2+8^2+9^2+1^2+17^2+3^2+9^2+21^2+29^2+11^2)}{3 \cdot 10}} = 8.12 \text{ seconds} \quad [21]$$

433 This value (8.1 seconds of arc) is very close to the *a posteriori* standard deviation of a  
 434 measurement of unit weight (8 seconds of arc for the measured angles) of the least  
 435

436 squares adjustment, which clearly indicates that the surveying methods of 1929 were  
437 appropriate and the quality of the angular observations (i.e. directions) was high.

438 The coordinate values in Tables 1 and 3 deserve an explanation with regard to the  
439 geodetic reference system. The coordinates in Table 3 differ from those of the Tissot  
440 projection system (Table 1) that was common in Spain in 1929. Instead, the station A  
441 was given arbitrary, local coordinates ( $X = 20000$ ,  $Y = 40000$ ) ensuring that the origin of  
442 the coordinate system falls southwest of the entire surveyed area (Table 2). A major  
443 drawback of this project, was that the project files contained information on a geodetic  
444 network that was eventually not used by the engineers. The choice of setting an  
445 arbitrary coordinate origin, however, agrees with recommendations for the set-up of  
446 urban grid systems in the absence of reliable higher order networks. For instance,  
447 Blachut et al. (1979) state that ‘the plain coordinate system for each urban community,  
448 or group of communities, should be designed so as to fulfill the particular needs of that  
449 community, even if this means a departure from an otherwise accepted regional  
450 coordinate system.’ The coordinates in the false origin system are referred to as  $X_{1929}$   
451 and  $Y_{1929}$ .

#### 452 ***4.4 Coordinate transformations***

453 The result of the transformation of the adjusted coordinates ( $X$ ,  $Y$ ) of Table 3 to  
454 ETRS89 is another interesting finding. It actually provides an insight into the geometric  
455 quality of the 1929 survey. As we progressed in our research, we realised that the  
456 original observations gave very consistent results and we expected a good agreement in  
457 rotation and scale when transforming the data of Table 3 into the ETRS89 system.

458 We carried out the transformation with two points in mind. First, we chose the  
459 affine transformation (Eqs. (14)-(19)) among many possible candidates because it does  
460 not constrain scale and rotation, which facilitates posterior interpretation. This

461 transformation uses six parameters that can be converted to a differential rotation  
462 representing the lack of perpendicularity between the axes ( $\epsilon$ ), a rotation angle ( $\theta$ ), and  
463 two scale factors, one for each of the two axes ( $SF_x, SF_y$ ).

464 The second point refers to the definition of the source and target coordinate  
465 systems and the agreement between them. As stated above, the 1929 coordinate  
466 reference system was defined as a plane, rectangular 2D system with an arbitrary origin  
467 and an orientation by astronomic methods. The ETRS89 was defined using GNSS  
468 techniques and geographic coordinates that are not compatible with plane coordinates.  
469 Therefore, we converted the geographical coordinates into two different target  
470 coordinate systems.

471 [Table 4 near here]

472 The first target system was the so-called local vertical coordinate (LVC) system,  
473 whose origin can be arbitrarily selected by the user (Wolf et al. 2014). It is worth noting  
474 here that the horizontal component (X, Y) of this coordinate system is, in many aspects,  
475 quite the same as the 2D plane system of 1929. The LVC coordinates are given in Table  
476 4.

477 The second system is the well-known Universal Transverse Mercator (UTM)  
478 cylindrical projection which is widely used in urban and large scale mapping (Blachut et  
479 al. 1979). The UTM grid defines a 2D rectangular system but the coordinates are  
480 affected locally by several elements of the projection such as the grid convergence and  
481 the point scale factor (Iliffe & Lott 2008, Snyder 1987). The UTM coordinates of Table  
482 4 are in Zone 30.

483 Table 5 shows the residuals of the affine transformations of the 1929 coordinates  
484 ( $Y_{1929}$  and  $Y_{1929}$  in Table 4) for all nine control points. The figures in both  
485 transformations are very similar. There are seven control points with residuals equal to

486 or less than 30 cm in the LVC transformation and six in the UTM transformation. We  
487 found residual vectors ranging from 4 cm to 65 cm (LVC) and from 3 cm to 63 cm  
488 (UTM) respectively. These large differences suggest that the use of more localised  
489 transformations would be beneficial to reduce the residuals of the transformation.  
490 Although this would be interesting, it is outside of the scope of this study.

491 [Table 5 near here]

492 The average residual  $s_0$  for each transformation is another precision criterion which can  
493 be calculated from the residuals of the least squares solution of the affine transformation  
494 (Table 5):

$$s_0 = \sqrt{\frac{r_x^2 + r_y^2}{2 \cdot n - p}} \quad [22]$$

495 where n is the number of control points (n=9) and p the number of parameters (p=6) of  
496 the transformation.

497 The average values are 0.260 m and 0.255 m for the 1929-LVC and 1929-UTM  
498 transformations respectively, showing very similar residual behaviour in both cases. It is  
499 worth noting that these average values include the larger error vectors of 0.65 m for  
500 ‘Grao’ in the two transformations under study.

501 Some geometric parameters of the transformations, namely scales and rotations  
502 in X and Y, are shown in Table 6. For the LVC transformation, a perfect fit would give  
503 a value of 1.0 for the scale factors and a value of 0.0 degrees for the rotation and  
504 perpendicularity angles. Regarding the LVC system, the scale factors are very close to  
505 the unit value, the rotation angle  $\theta$  of the X axis is -0.024253 degrees (1'27''), and the  
506 perpendicularity angle  $\epsilon$  is 0.007595 degrees (27 seconds of arc). These values prove  
507 the great performance of the invar wire and astronomical orientation techniques.

508 [Table 6 near here]

509 When considering the UTM parameters, it is clear that the UTM scale factor and the  
 510 UTM grid convergence mask the fit between the 1929 and the UTM spaces. In order to  
 511 account for the influence of the projection on the transformation parameters we  
 512 computed the nominal UTM values (point scale factor and grid convergence) of the  
 513 central point Miguelete II of the study area and corrected the raw UTM transformation  
 514 parameters.

515 The UTM nominal values for Miguelete II are:

516 Latitude: 39° 26' 33.79'' N

517 Longitude: 0° 20' 07.36'' W

518 Point scale factor: 1.00024744

519 Grid convergence: -1° 41' 37'' ~ -1.693611 deg

520 Regarding the scale factors, it is worth noting that in the 1929-LVC transformation, they  
 521 can be considered 'true scale factors' in the sense that they connect two pure Cartesian  
 522 systems. In the 1929-UTM transformation, however, the nominal UTM scale factor  
 523 affects the experimental scale factors so that they cannot be directly compared to their  
 524 1929-LVC counterparts. In order to do that comparison properly, we applied the UTM  
 525 nominal scale factor as follows:

$$SF'_x = \frac{1.000143}{1.00024744} = 0.999896 \quad [23]$$

$$SF'_y = \frac{1.000205}{1.00024744} = 0.999957 \quad [24]$$

526 where  $SF'_x$  and  $SF'_y$  are the corrected scale factors which are similar to those of the  
 527 1929-LVC transformation. Note that scale factors may also be computed in units of



528 ppm by subtracting the computed and nominal values which gives -104 ppm (1.000143-  
529 1.000247) for  $SF'_X$  and -42 ppm (1.000205-1.000247) for  $SF'_Y$ .

530 The influence of the grid convergence angle is larger since it is 'embedded' in the target  
531 reference system. Furthermore, the affine transformation formulas do not provide  
532 mechanisms to separate convergence from true rotation either, so that we have to  
533 correct for that convergence after computing the transformation. The result is a  
534 corrected rotation angle for the  $x$ -axis after a summative operation:

$$\theta' = 1.645097 - 1.693611 = -0.048514 \text{ degrees} = -2'55'' \quad [25]$$

535 This corrected value is now much smaller and about double the  $\theta$  angle in the 1929-  
536 LVC transformation.

537 The results of the scale and rotation analyses suggest that the LVC system works  
538 slightly better than the UTM system in geometric terms, even after correcting the UTM  
539 parameters. However, in common practice, the LVC system is rarely used in large scale  
540 and urban mapping, and the UTM projection system is preferred. Be that as it may, the  
541 UTM results are suitable to transform the 1929 map into modern reference systems and  
542 integrate the 1929 map with digital databases. The relevant parameters ( $A$  to  $F$ ) of the  
543 affine transformation are listed in Table 6.

544 Another finding of the study was the exact location of the Miguelete I station  
545 used in the 1929 project. In the current Spanish national geodetic network there is a first  
546 order station called Miguelete. It was not clear whether those two stations were identical  
547 or in two close, but different locations. We confirmed that they were two different  
548 stations when we calculated the transformation between the 1929 local and the ETRS89  
549 coordinates.

550 Figure 7 shows three different points on the rooftop of the tower. The station  
551 Miguelete I is shown by an empty triangle with a central dot and the current first order  
552 station Miguelete with a red, solid triangle on the western half of the tower (above the  
553 ‘e’ of ‘del’). The other solid triangle on the eastern half is Miguelete II (above the ‘t’ of  
554 ‘Micalet’), which was also used in the 1929 project and is still marked on the tower  
555 roof. The resolution of the issue of the Miguelete I station was important for the  
556 determination of the geodetic coordinate reference system for the project.

557 [Figure 7 near here]

## 558 **5. Conclusions**

559 In this paper we examined the geometric and cartographic characteristics of the  
560 triangulation network used to make the first 1:500 urban map of València. The study  
561 involved bibliographic work, field trips, and computer programming in a demanding  
562 research effort. As a result, we gained considerable insight into the fundamentals of the  
563 observational and computational processes of the network that were originally  
564 conducted almost one century ago.

565 The quality and detail of the original survey documentation allowed us to  
566 reprocess the original data. The least squares processing of the original angular  
567 observations showed that the standard deviations of the measured angles and the  
568 adjusted coordinates were very satisfactory.

569 The affine transformations based on a set of points of the original network and  
570 GNSS observations were used to convert the 1929 data into modern coordinate  
571 reference systems. The scale and rotation parameters of the affine transformations  
572 demonstrated the accuracy of the invar wire length measurements and the astronomic  
573 orientation of the baselines.

574           Although the plane coordinate system of the 1929 network is local, the  
575 fieldwork and computations conducted in this study allow us to integrate the urban map  
576 with modern spatial databases stored in global coordinate systems. There are many  
577 applications of such data integration in the regular operation of City Survey Offices as  
578 well as in cadastral and urban planning services. In the case of the València City  
579 Council, the 1929 map has been used in several legal matters. In summary, the map of  
580 1929 is a cartographic gem that can now be integrated with other municipal spatial  
581 databases for urban planning, cadastral and even legal purposes.

## 582 **Acknowledgements**

583 We would like to thank former Prof. Manuel Chueca, founder of the School of Geodesy,  
584 Cartography, and Surveying Engineering at the Universitat Politècnica de València in Spain, for  
585 providing bibliographic materials and a unique insight into the map of 1929. We also thank the  
586 staff at the València City Council for their kindness, help, and support, especially Ms Cristina  
587 Sigalat and Mr Juan Sáiz. Finally, a great debt of gratitude is owed to an anonymous reviewer  
588 who provided key insights and helped the authors shape the early drafts of the paper into its  
589 final form.

## 590 **References**

- 591 Bennett G.G., & Freislich, J.G., 1979. *Field Astronomy for Surveyors*. Kensington: New South  
592 Wales University Press. 249 pages.
- 593 Benoît J.R., & Guillaume, C.E., 1917. *La mesure rapide des bases géodésiques* [Fast  
594 measurement of geodetic baselines]. Paris: Gauthier-Villars. 228 pages. (In French).
- 595 Bitelli, G., Cremonini, S., & Gatta, G., 2014. *Cartographic heritage: Toward unconventional*  
596 *methods for quantitative analysis of pre-geodetic maps*. *Journal of Cultural Heritage* 15,  
597 183-195.
- 598 Bomford G., 1952. *Geodesy*. London: Oxford University Press. 447 pages.
- 599 Blachut T.J., Chrzanowski A., & Saastamoinen J.H., 1979. *Urban Surveying and Mapping*.  
600 New York, NY: Springer-Verlag. 365 pages.
- 601 Brinker, R.C., & Minnick, R., 1987. *The Surveying Handbook*. New York, NY: Springer  
602 Science+Business Media. 1248 pages.
- 603 Cebrián, P., & Los Arcos, A., 1895. *Teoría General de las Proyecciones Geográficas y su*  
604 *Aplicación a la Formación de un Mapa de España* [General theory of geographic  
605 projections and its application to making a map of Spain]. Madrid: Dirección General  
606 del Instituto Geográfico y Estadístico. 278 pages. (In Spanish).
- 607 de la Puente, J.M., 1925. *La medida de bases con hilos 'Invar' en el plano del Extrarradio de*  
608 *Madrid* [Baseline measurement with Invar wires in the Madrid outskirts map].  
609 *Ingeniería y Construcción*, 3 (30), 254-256. (In Spanish).
- 610 Clark, D., 1948. *Plane and Geodetic Surveying*. 4th Ed. London: Constable & Company LTD.  
611 481 pages.

- 612 Gatta, G., 2010. *Valorizzazione di cartografia storica attraverso moderne tecniche geomatiche:*  
613 *recupero metrico, elaborazione e consultazione in ambiente digitale* [Valuation of  
614 historic cartography using modern geomatics techniques: metric recovering, making and  
615 use in digital environment]. Doctoral thesis. Bologna: Università di Bologna. 295 pages.  
616 (In Italian).
- 617 Gorse, C., Johnston D., & Pritchard M., 2012. *Dictionary of Construction, Surveying & Civil*  
618 *Engineering*. Oxford: Oxford University Press. 506 pages.
- 619 Haasbroek, N.D., 1968. *Gemma Frisius, Tycho Brahe and Snellius and their triangulations*.  
620 Delft: Netherlands Geodetic Commission. 116 pages.
- 621 Hewitt, R., 2011. *Map of a nation: a biography of the Ordnance Survey*. London: Granta  
622 Books. 432 pages.
- 623 Hotine, M., 1939. *The re-triangulation of Great Britain—IV. Base Measurement*. Empire  
624 Survey Review, 5:34, 211-225, DOI: 10.1179/sre.1939.5.34.211  
625
- 626 IGC, 1928. *Anuario del Observatorio astronómico de Madrid*. [Almanac of the Madrid  
627 Astronomic Observatory] Madrid: Instituto Geográfico y Catastral. 488 pages. (In  
628 Spanish).
- 629 IGE, 1907. *Instrucciones para los trabajos topográficos*. [Instructions for surveying works].  
630 Madrid: Dirección General del Instituto Geográfico y Estadístico. 314 pages. (In  
631 Spanish).
- 632 Ilife, J.C., & Lott, R., 2008. *Datums and Map Projections for remote sensing, GIS and*  
633 *surveying*. Caithness: Whittles Publishing. 150 pages.
- 634 Kahmen, H. & Faig, W., 1988. *Surveying*. Walter de Gruyter: Berlin, London. 602 pages.
- 635 Kennie, T.J.M., & Petrie, G., 2010. *Engineering Surveying Technology*. London: Taylor and  
636 Francis. 489 pages.
- 637 Leick, A., Rapoport, L., & Tatarnikov, D., 2015. *GPS satellite surveying*. Hoboken, NJ: Wiley.
- 638 Mugnier, C.J., 2000. *Grids and Datums. The kingdom of Spain*. Photogrammetric Engineering  
639 and Remote Sensing, 66 (4), 813-814. 840 pages.
- 640 Murdin, P., 2010. *Full meridian of glory*. New York, NY: Springer-Verlag. 162 pages.
- 641 Navarro, V., 2004. *Jerónimo Muñoz. Introducción a la Astronomía y la Geografía* [Jerónimo  
642 Muñoz. Introduction to Astronomy and Geography]. Valencia: Conselleria Valenciana  
643 de Cultura. 354 pages. (In Spanish).
- 644 Nobel Foundation, 1998. *Nobel lectures in Physics 1901-1921*. Singapore: World Scientific.  
645 510 pages.
- 646 Roselló, V., 2000. *Jerónimo Muñoz y la primera Triangulación Valenciana* [Jerónimo Muñoz  
647 and the first Valencian triangulation]. Valencia: Universitat de Valencia. (In Spanish).
- 648 Roselló, V., 2008. *Cartografía histórica dels Països Catalans* [Historic cartography of the  
649 Catalan countries]. Illes Balears: Universitat de les Illes Balears. 401 pages. (In  
650 Catalan).
- 651 Schofield, W., & Breach M., 2007. *Engineering Surveying*. 6<sup>th</sup> Ed. Oxford: Elsevier. 622 pages.
- 652 Schrön, L., 1893. *Tables de Logarithmes a Sept Décimales* [Logarithm tables with  
653 sevendecimal places]. Paris: Gauthier-Villars. 478 pages. (In French).
- 654 Seeber, G., 2003. *Satellite Geodesy: foundations, methods, and applications*. New York, NY:  
655 Walter de Gruyter. 575 pages.
- 656 Shank, V., 2012. *Surveying Engineering & Instruments*. Delhi: White Word Publications. 105  
657 pages.
- 658 Snyder, J.P., 1987. *Map projections - A working manual*. NW, Washington, D.C.: United States  
659 government printing office. 377 pages.
- 660 Strang, G., & Borre, K., 1997. *Linear algebra, geodesy and GPS*. Delhi: Wellesley-Cambridge  
661 Press. 640 pages.
- 662 Tissot, M.A., 1881. *Mémoire sur la Représentation des Surfaces et les Projections des Cartes*  
663 *Géographiques* [Report on the representation of surfaces and map projections]. Paris:  
664 Gauthier-Villars. (In French).
- 665 Wolf, P.R., Dewitt, B.A., & Wilkinson, B.E., 2014. *Elements of Photogrammetry with*  
666 *Applications in GIS*. New York, NY: McGraw-Hill. 696 pages.



668 Table 1. Computed Tissot coordinates and differences from the published Tissot  
 669 coordinates of 1929

670	<b>Station</b>	<b>X<sub>COMP</sub> (m)</b>	<b>Y<sub>COMP</sub> (m)</b>	<b>X<sub>PUBL</sub> (m)</b>	<b>Y<sub>PUBL</sub> (m)</b>	<b>ΔX (m)</b>	<b>ΔY (m)</b>
671	Rebalsadores	877312.65	571584.17	877312.30	571584.14	0.35	0.03
672	Cullera	896560.14	514338.09	896559.61	514338.07	0.53	0.02
673	Faro	898140.52	569714.64	898140.20	569714.62	0.32	0.02

674

675 Table 2. Coordinates of the terminals *A*, *B*, *C* and *D* of the two baselines *AB* and *CD*  
 676 defining the 1929 local coordinate system

	<b>Station</b>	<b>X<sub>1929</sub> (m)</b>	<b>Y<sub>1929</sub> (m)</b>
	A	20000.00	40000.00
	B	19666.57	40384.44
	C	27659.42	24889.63
	D	27740.30	24371.39

677

678 Table 3. Approximate coordinates (*X<sub>A</sub>*, *Y<sub>A</sub>*), adjusted coordinates (*X*, *Y*), and standard  
 679 deviations of the adjusted coordinates *s<sub>X</sub>* and *s<sub>Y</sub>*. Coordinates in the 1929 local  
 680 coordinate system

681

682	<b>Station</b>	<b>X<sub>A</sub>(m)</b>	<b>Y<sub>A</sub>(m)</b>	<b>X (m)</b>	<b>Y (m)</b>	<b>s<sub>X</sub> (m)</b>	<b>s<sub>Y</sub> (m)</b>
683	Benimamet	20225.56	37946.63	-----	-----	-----	-----
684	Burriel	21930.63	38069.11	21930.67	38069.09	0.023	0.071
685	Mislata	20310.29	35452.40	20310.27	35452.41	0.071	0.093
686	Miguelete I	23908.07	35473.72	-----	-----	-----	-----
687	Tormo	22563.03	33613.49	22563.02	33613.46	0.098	0.083
688	S. Luis M	24720.81	32034.10	24720.89	32034.07	0.187	0.162
689	Almácer	25616.76	39589.87	25616.86	39589.83	0.171	0.162
690	Miguelete II	23915.46	35480.59	-----	-----	-----	-----
691	Malvarrosa	27994.72	36417.30	27994.73	36417.15	0.179	0.202
692	Grao	27488.37	33846.34	27488.30	33846.17	0.237	0.166
693	S. Luis M II	24723.88	32034.15	24723.73	32034.20	0.237	0.166
694	Sancho	27377.67	31860.15	27377.41	31860.07	0.289	0.259
695	Castellar	24961.98	30377.44	24961.90	30377.43	0.355	0.232

696

697 Table 4. Coordinates of the stations used in coordinate transformations (UTM  
698 coordinates in zone 30).  $X_{1929}$ ,  $Y_{1929}$  are the 1929 published coordinates in the local  
699 coordinate system. The UTM and LVC target coordinates were converted from the  $\phi, \lambda$   
700 of the new GPS survey

Station	$X_{1929}$ (m)	$Y_{1929}$ (m)	$X_{UTM}^a$ (m)	$Y_{UTM}^a$ (m)	$X_{LVC}$ (m)	$Y_{LVC}$ (m)
Benimamet	20225.56	37946.63	721973.321	4375175.925	-3688.540	2467.358
Mislata	20310.29	35452.40	722139.615	4372684.928	-3604.900	-26.661
Almácer	25616.76	39589.87	727326.543	4376970.213	1703.719	4108.799
Miguelete 2	23915.46	35480.59	725740.934	4372816.608	0.000	0.000
Sancho	27377.67	31860.15	729318.691	4369282.395	3459.953	-3621.696
Grao	27488.37	33846.34	729361.254	4371284.690	3571.367	-1636.282
Castellar	24961.98	30377.44	726935.213	4367744.983	1043.888	-5103.069
Puente del Mar	25029.35	34925.50	726870.327	4372293.579	1113.434	-555.580
Pechina	22514.06	35662.39	724350.668	4372923.164	-1401.247	182.420

701

702

703

704 Table 5. Residuals of the coordinate transformations of the 1929 coordinates ( $X_{1929}$ ,  
705  $Y_{1929}$  of Table 3) to the LVC ( $X_{LVC}$ ,  $Y_{LVC}$  in Table 4) and UTM spaces ( $X_{UTM}$ ,  $Y_{UTM}$  in  
706 Table 4)

Station	1929 to LVC			1929 to UTM (Zone 30)		
	$r_X$ (m)	$r_Y$ (m)	$\sqrt{r_X^2 + r_Y^2}$ (m)	$r_X$ (m)	$r_Y$ (m)	$\sqrt{r_X^2 + r_Y^2}$ (m)
Benimamet	-0.2242	-0.1985	0.2994	-0.2040	-0.2615	0.3317
Mislata	0.0684	0.0148	0.0700	0.0927	0.0410	0.1013
Almácer	0.2707	0.3129	0.4138	0.2196	0.3361	0.4015
Miguelete 2	0.0628	0.0024	0.0628	0.0581	0.0213	0.0619
Grao	-0.3641	-0.5353	0.6474	-0.3038	-0.5504	0.6287
Sancho	0.0191	0.1590	0.1602	0.0423	0.1187	0.1260
Castellar	0.2164	0.2178	0.3071	0.1478	0.2382	0.2804
Puente del Mar	-0.0406	-0.0158	0.0436	-0.0327	-0.0019	0.0327
Pechina	-0.0087	0.0427	0.0435	-0.0200	0.0585	0.0618

707

708

709  
 710 Table 6. Geometrical parameters of the affine transformations from the published 1929  
 711 coordinates in the local coordinate system (columns 2, 3 in Table 4) to the GPS derived  
 712 UTM (columns 4, 5 in Table 4) and LVC (columns 6, 7 in Table 4) systems

<b>Parameter</b>	<b>LVC</b>	<b>UTM</b>
$SF_X$	0.999933	1.000143
$SF_Y$	0.999983	1.000205
$\epsilon$ (degrees)	0.007595	0.007705
$\theta$ (degrees)	-0.024253	1.644985
A	0.999933	0.999731
B	0.000556	-0.028578
D	-0.000423	0.028711
E	0.999983	0.999797
C (m)	-23933.622	702845.845
F (m)	-35469.863	4336656.581

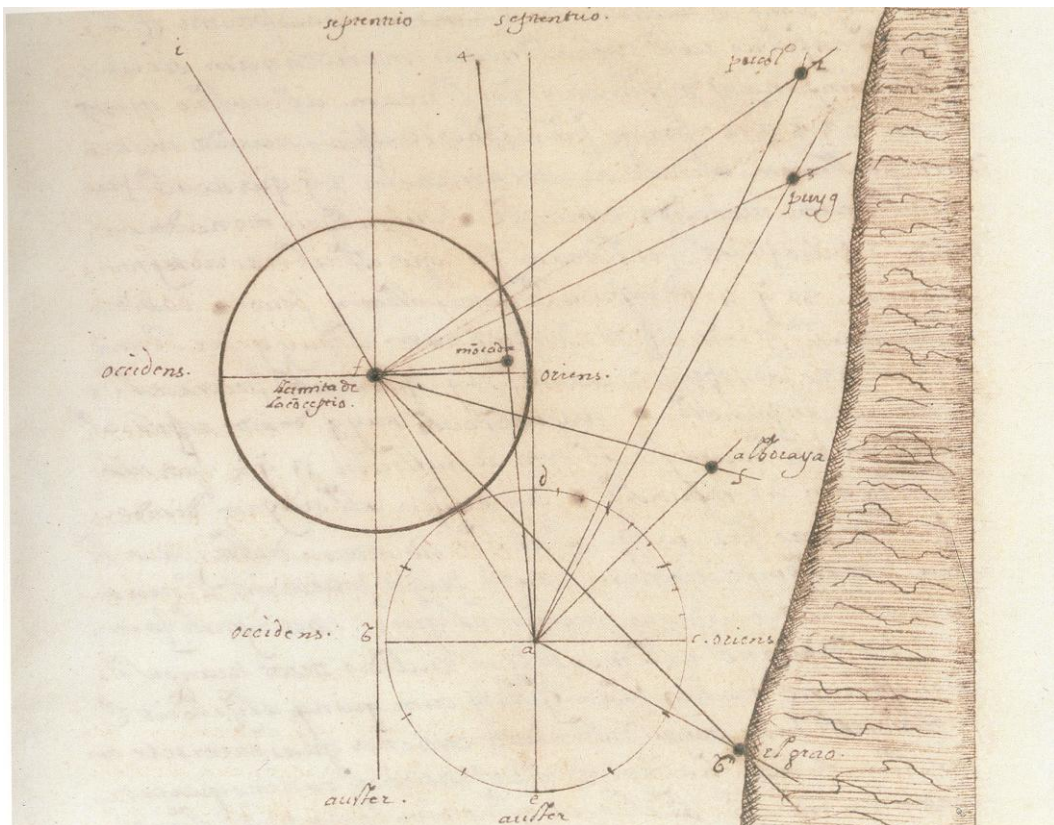
713



714 Figure 1  
715

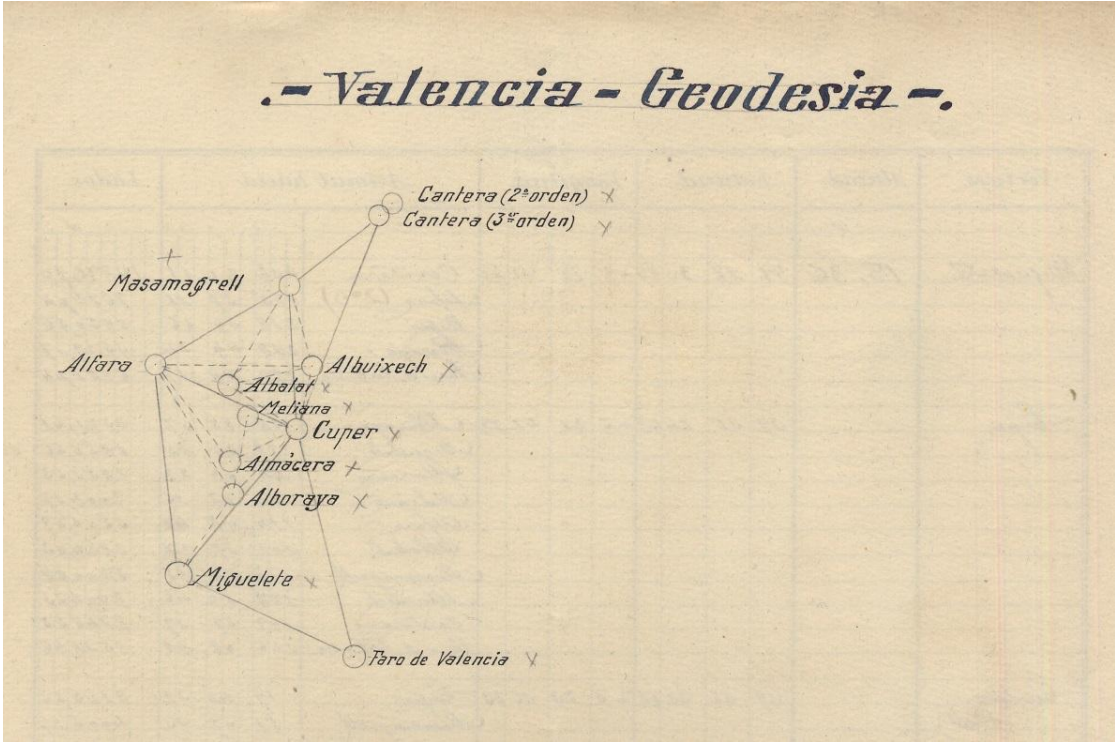


716  
717  
718  
719  
720 Figure 2  
721



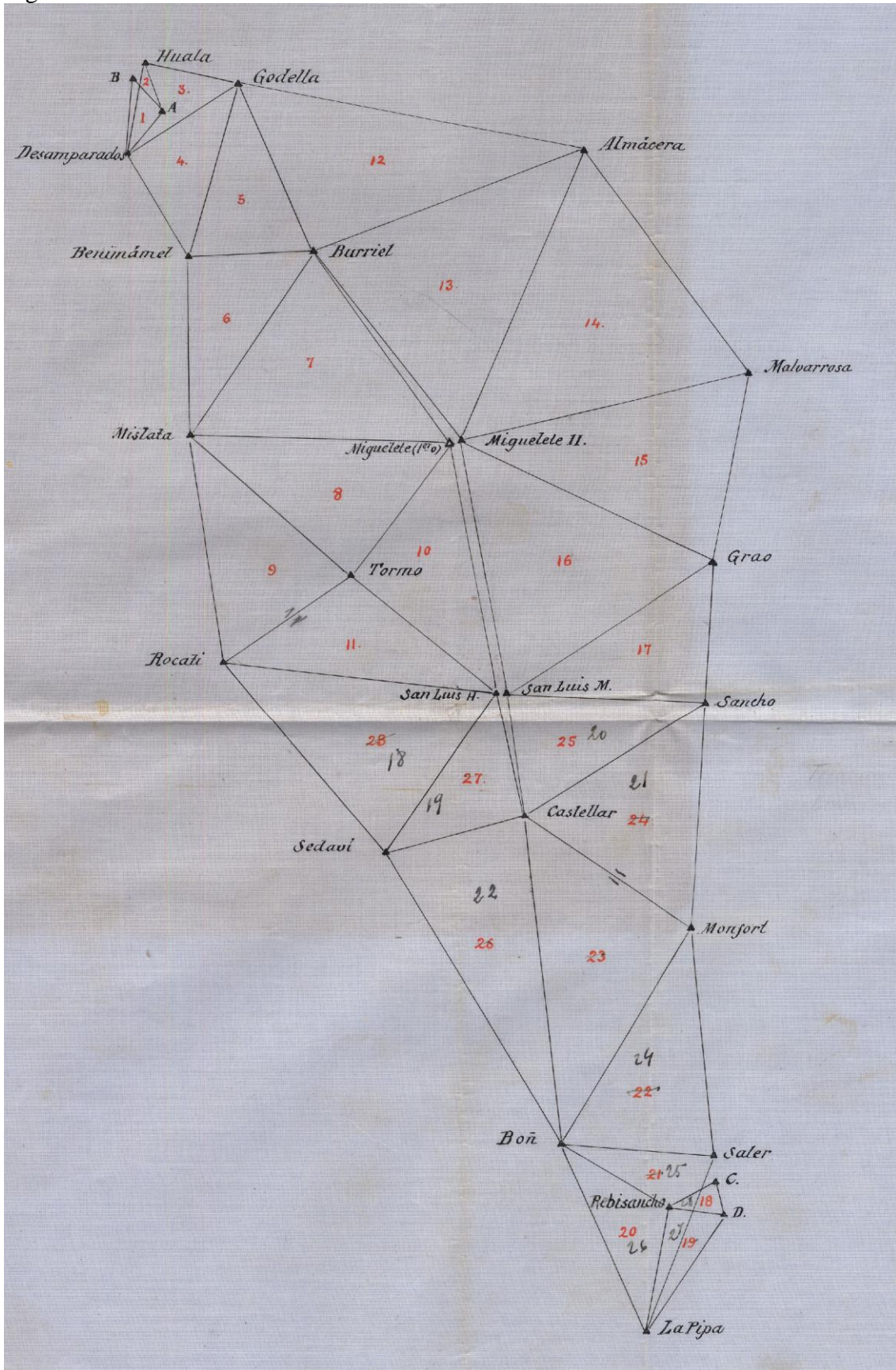
722  
723  
724  
725  
726  
727  
728 Figure 3

729



730  
731

732 Figure 4



733  
734

*Se ve* I. Aljuel de la Reina I y II  
 Echona Blanque (parral)  
 Marqués (Echona)  
 Luján (Echona)  
 Luján (Echona)  
 Luján (Echona)  
 Luján (Echona)  
 Luján (Echona)  
 Luján (Echona)

Castillo  
 Rincón (A)  
 Bonasa Carolina Boncepa  
 Carrera San Abad  
 Alcantarilla  
 Alcantarilla (A)  
 Corral de la Cruz (pueblo)

**Vértice Almácer**

Situado en la provincia de **Valencia** término de **Almácer**

en **el centro del penúltimo piso de la torre de la Iglesia del pueblo de su nombre.**

El itinerario para llegar a este punto desde el pueblo de **Valencia** del que dista **1/2** horas, es el siguiente: **en tren a Almácer**

*Mod. T. 4 a.*

Señalado con un taladro cilíndrico de ..... centímetros de profundidad y ..... de diámetro, relleno de polvo de carbón, en cuyo fondo se clavó una estaca y referido a otras tres ..... en la forma que indica el croquis; fué cubierto con un montón de tierra y piedras, en forma de pirámide triangular, de un metro de lado en su base y 0,50 de altura, habiéndose pintado de negro en una de sus caras un triángulo equilátero.

*ante del*

*Cometa*

Corte de la torre (Croquis.)

Campana

1,78 1,77 1,73

1,79 1,26 1,91 3,10

739 Figure 6  
740



(a)

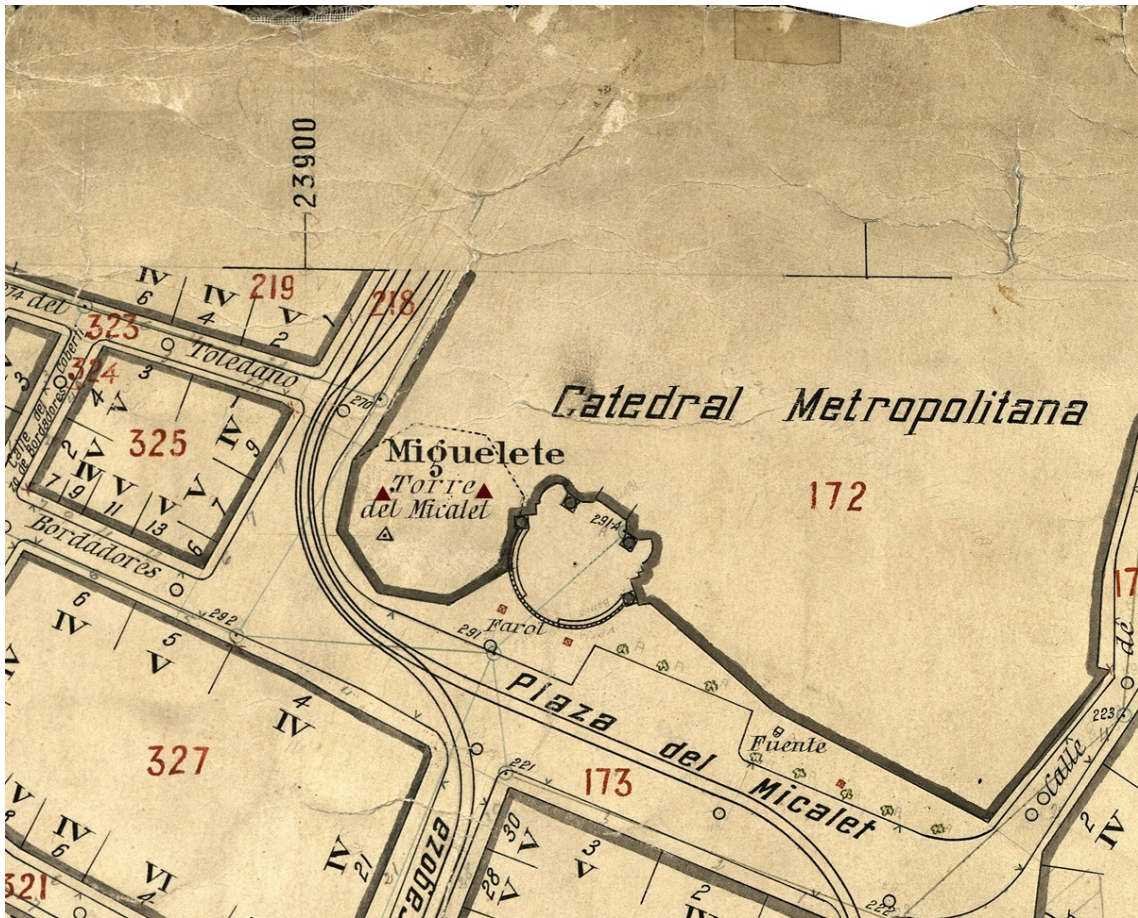


(b)

741  
742

743 Figure 7

744



745

746

747 Figure 1. Location of the city of València in Spain (North towards top of figure).

748 Figure 2. Early triangulation draft by J. Muñoz on the Valencian coast (Navarro 2004).

749 Note the use of latin words for the cardinal points (*septentrio* [north], *auster* [south],

750 *oriens* [east], and *occidens* [west]) as usual at the time (North towards top of figure).

751 Figure 3. Scketch of the network used to connect the 1929 urban network with the

752 Spanish national geodetic network. North is upwards. The distance from ‘Cantera’ to

753 ‘Faro de Valencia’ is about 15 km.

754 Figure 4. Original plan of the urban primary triangulation of 1929 (North-South: 13.4

755 km, East-West: 7.7km). Note the strategic locations of the baselines *AB* and *CD* at the

756 limits (S, N) of the surveyed area (North upwards).

757 Figure 5. Point description of the station Almacera. The recovery scketches at the

758 bottom of the form allow the relocation of the point, if necessary.

759 Figure 6. Original mark of the station Benimàmet (a) and the GNSS antenna during our

760 resurvey (b).

761 Figure 7. Sample of the 1929 map with the location of the points Miguelete (upper left,

762 red triangle), Miguelete I (bottom left, empty triangle with central dot) and Miguelete II

763 (upper right, red triangle). Note that the unlabelled grid line in the upper-right area (over

764 the ‘r’ in ‘Metropolitana’) that corresponds to the X coordinate 23950.